Journal of Solid State Chemistry **146,** 245–252 (1999)
Article ID jssc.1999.8345, available online at http://www.idealibrary.com on IDEAL®

Structure of Highly Divided Nonstoichiometric Iron Manganese Oxide Powders $Fe_{3-x}Mn_x\square_{3\delta/4}O_{4+\delta}$

Sophie Guillemet-Fritsch,[1] Sophie Viguié, and Abel Rousset

Laboratoire de Chimie des Matériaux Inorganiques et Enginétiques, ESA CNRS 5070, Université Paul Sabatier-Bâtiment 2R1-118, Route de Narbonne, 31062 Toulouse Cedex, France

Received November 25, 1998; in revised form April 5, 1999; accepted April 22, 1999

Highly divided iron manganese oxide powders, $Fe_{3-x}Mn_x\square_{3\delta/4}O_{4+\delta}$, were prepared at low temperature ($T \leq 560°C$) by the thermal decomposition of mixed oxalate precursors $Fe_{1-\alpha}Mn_\alpha C_2O_4$, $2H_2O$ ($\alpha = x/3$). The manganese-rich compounds ($x \geq 1.5$) have a complex structure that can be cubic, tetragonal, or a mixture of both tetragonal and cubic spinel phases that indicates a lack of miscibility existing in the Fe_3O_4–Mn_3O_4 phase diagram at low temperature. The structure strongly depends on the chemical composition but also on the nonstoichiometric coefficient (δ). It has been identified as one of the mineral "vredenburgite" and has never been reported before for powders prepared by chimie douce. The oxygen excess, determined by thermogravimetric analyses, is the highest ($\delta = 0.4$) when the oxide is prepared at 410°C. Theses oxides are defect spinel phases containing cationic vacancies.

INTRODUCTION

Manganese iron oxides have been the subject of many research works due to their potential applications to magnetic recording media and electronic devices. In these systems, the cation distribution, the oxygen content, and therefore their specific properties are largely influenced by the preparation conditions.

The phase diagram of the Fe/Mn/O system is well known at high temperature (1–7). The spinel phase is obtained in air at temperatures above 950°C. The structure can be cubic or tetragonal, depending on the composition. In fact, if the quantity of Mn^{3+} cations is higher than 1.8 per 4 oxygen cations (1, 8), then the spinel structure transforms from cubic to tetragonal, due to the cooperative Jahn–Teller effect on Mn^{3+} cations. The few structural studies realized on this system calcined at temperatures below 500°C did not allow the identification of the phases because of the poor crystallinity of the samples (9, 10).

[1]To whom correspondence should be addressed. E-mail: fritsch@ramses.ups-tlse.fr.

The cubic-to-tetragonal phase transition has mainly been described as a diffusionless reaction. However, Cerkinka *et al.* (11) have pointed out a tetragonal microdomain structure in a cubic matrix. In general, the coexistence of cubic and tetragonal spinel phases have been rarely been mentioned in the literatue, especially at low temperature. Muan and Somiya (4) have shown the existence of a phase mixture for temperatures higher than 950°C. In a similar way, the phase diagram of Mason (1) shows that two phases coexist at high temperature for a composition ranging from $Fe_{0.15}Mn_{2.85}O_4$ to $Fe_{0.45}Mn_{2.55}O_4$. Annealing experiments (12) performed on the $Fe_{3-x}Mn_xO_{4+\delta}$ system at 940°C have permitted the determination of the equilibrium miscibility limits. However, the same authors (12) indicate that, at temperatures below 700°C, the very low reaction rate makes reaching equilibria under laboratory conditions difficult. Then, the only limits which can be taken as corresponding to equilibrium are those deduced from natural "vredenburgite." Mason (1) has reported a complete description of vredenburgite. This mineral naturally contains a mixture of cubic and tetragonal spinel phases. It corresponds to the immiscibility gap at low temperature in the Fe_3O_4/Mn_3O_4 diagram for the compositions comprised between $Fe_{1.35}Mn_{1.65}O_4$ and $Fe_{0.27}Mn_{2.73}O_4$. The mineral was described as an intergrowth of the minerals jacobsite ($MnFe_2O_4$) and hausmannite (Mn_3O_4). The structure is typical of an exsolution appearing during the cooling procedure of a mixed crystal elaborated at high temperature.

In the past 10 years, highly divided particles of different substituted ferrites have been prepared by "chimie douce" at low temperature. They are mixed valence defect oxides (13–15) and are described as a "new family" of ferrites, having specific characteristics and properties. In the Fe/Mn/O system, the structure of the phases that have been prepared at low temperature has been studied for iron-rich compounds, the manganese ferrites (16–21). Only one work (19) describes some structural characteristics of Mn/Fe spinel oxides prepared by thermal decomposition of mixed carbonates. However, the present work will show that the

0022-4596/99 $30.00

structure of this system is even more complex than the one described in (19).

The aim of this study is to prepare and characterize highly divided iron manganese oxide powders having the spinel structure. The oxides are obtained by the thermal decomposition of the mixed oxalate precursors. The characterizations will be done by XRD, TGA, and TEM.

EXPERIMENTAL

The oxalate precursors are obtained by the co-precipitation of iron and manganese chlorides with oxalic acid, according to Eq. [1]:

$$(1-\alpha)\,FeCl_2,\,4H_2O + \alpha MnCl_2,\,4H_2O + H_2C_2O_4,\,H_2O \rightarrow Fe_{1-\alpha}Mn_\alpha C_2O_4,\,xH_2O + 2Cl^- + 2H^+ + (5-x)H_2O. \quad [1]$$

The oxalic acid is dissolved in an ethanol solution of concentration 0.4 M, which corresponds to the solubility limit at ambient temperature. The dissolution has to be made just before the coprecipitation reaction is started to avoid the formation of an ester. The metallic salts are dissolved in a water/alcohol medium (concentration 2 M). The salts are introduced quickly in the acid solution so as to favor the germination phenomenon in comparison with the growth. The precipitates are filtered, washed with distilled water, and dried at 80°C overnight. The thermal decomposition of the precursors is realized under a controlled atmosphere of flowing gas (a mixture of nitrogen and air). The flow rate of each gas has to be optimized to get the pure spinel phase at low temperature: the flow rate of air is 6 L/h and that of nitrogen is 250 L/h. The heating rate is first fixed at 150°C/h up to $(T-30)$°C and then decreased to 60°C/h up to the dwell temperature T (3 h). The cooling rate is 150°C/h.

TEM observations were performed using a HITACHI 300. The chemical analyses are determined using atomic absorption spectroscopy. Additional local analyses were done using a microprobe, associated to a JEOL 2010 TEM. The smallest diameter of the probe is 1.5 nm. The granulometric distribution is determined using a HORIBA CAPA 700 granulometer. X-ray powder diffraction patterns were collected on a SIEMENS D501 diffractometer, equpped with a Peltier effect counter using either the Co$K\alpha$ radiation ($\lambda = 0.17902$ nm) or the Cu$K\alpha$ radiation ($\lambda = 0.15418$ nm). TGAs were performed using a SETARAM TAG24 apparatus, in flowing air. Before the TG experiments, the powders are carefully degassed (0.5 Pa) at 100°C for 5 h to eliminate all the species that are absorbed at the surface of the samples. To make sure that no species remain adsorbed after the degassing procedure, the gas eliminated during the heating ramp was analyzed both by gas chromatography (SHIMADZU GC-81 chromatograph fitted with a molecular sieve 13 × column and a thermal conductivity detector) and by transmission IR Fourier transform spectrometry (Nicolet 510P IF-IR). These experiments show that no water molecules remain. Only the IR spectra indicate a very small signal of CO_2 gas (less than 0.005%) appearing between 150 and 300°C.

RESULTS AND DISCUSSION

The precursor powders have an octahedral-like shape and their size is approximately 0.1–0.5 μm. The granulometric analyses show that the distribution size of the powders is narrow. The size of the particles tends to increase with the manganese content. The oxalates, whatever their composition, are single phase and crystallize in an orthorhombic structure (Fig. 1), which is a metastable β phase, described by Lagier (22). It has been shown previously that this form generally appears when the coprecipitation is made in an alcoholic medium (23). The thermal behavior of the precursors was followed by TGA under air flow. Two reactions are observed during the heating ramp. At 110°C, the mass change is attributed to the loss of two water molecules, according to

$$Fe_{1-\alpha}Mn_\alpha C_2O_4,\,2H_2O \rightarrow Fe_{1-\alpha}Mn_\alpha C_2O_4 + 2H_2O. \quad [2]$$

The second reaction, observed at 220°C, is due to the decomposition of the oxalate group:

$$3Fe_{1-\alpha}Mn_\alpha C_2O_4 \rightarrow Fe_{3-x}Mn_xO_4 + 4CO + 2CO_2 \quad (\text{with } x = 3\alpha). \quad [3]$$

The decomposition reaction is over at 290°C.

The composition of the oxides is reported in Table 1, Together with the corresponding oxalates. The local analyses of iron and manganese elements, determined using the microprobe, indicate that the different grains are homogeneous in composition. The oxide particles have the same octahedral shape (Fig. 2) as the one of the precursors. The average size of the crystallites, evaluated from XRD line broadening using Scherrer's equation, varies between 10 and 50 nm for a temperature of calcination ranging from 410 to 530°C.

The structure of the oxides strongly depends on the composition. The iron-rich compounds $Fe_{3-x}Mn_xO_4$ ($x < 1.5$) are single phase and crystallize in the cubic spinel phase, for a temperature of calcination up to 560°C. At this temperature, two additional phases are observed in addition to the spinel phase, the cubic α-Mn_2O_3 and the rhombohedral hematite α-Fe_2O_3. The manganese-rich compounds ($x \geq 1.5$) are polyphased too at the same temperature (560°C). But only the cubic α-Mn_2O_3 phase is identified,

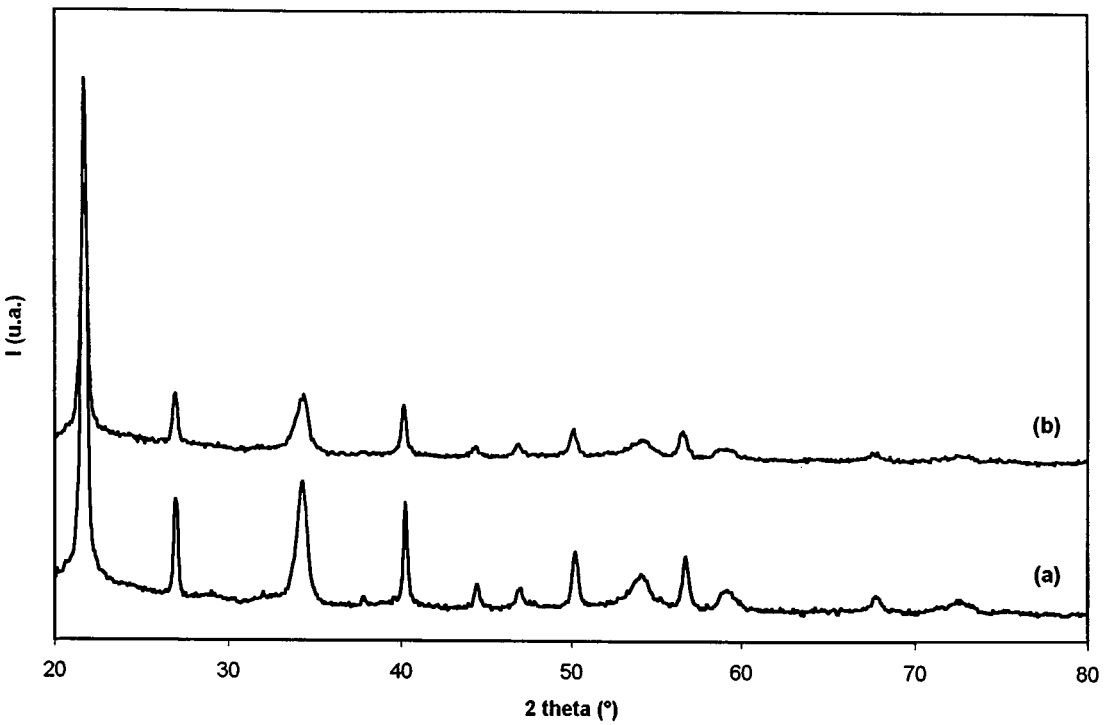

FIG. 1. X-ray diffraction pattern of mixed iron manganese oxalate precursors (a) $Fe_{0.87}Mn_{0.13}C_2O_4$, $2H_2O$ and (b) $Fe_{0.73}Mn_{0.27}C_2O_4$, $2H_2O$.

besides the spinel phase, indicating that the iron cations form a solid solution with the manganese cations. This phase can be written as α-$(Fe_{1-y}Mn_y)_2O_3$. In the case of manganites, the structure of the low-temperature spinel phase can be cubic, tetragonal, or a mixture of both cubic and tetragonal phases (Table 2). The ratio of the tetragonal phase increases as the manganese content increases. In fact, the distortion of the spinel phase which undergoes the cubic-to-tetragonal phase transition is due to the cooperative Jahn–Teller effect of the Mn^{3+} cations located on the octahedral sites. For the two oxides ($Fe_{1.32}Mn_{1.68}O_4$ and $Fe_{1.08}Mn_{1.92}O_4$) that are composed of a mixture of phases, the ratio of each phase is different at each temperature, which indicates that the oxidation state varies with temperature. The X-ray diffraction pattern of a manganite of composition $Fe_{1.32}Mn_{1.68}O_4$ prepared at 410, 430, 470, and 1050°C is reported in Fig. 3. For the same chemical

TABLE 1
Composition of the Oxalate Precursors and of the Corresponding Iron Manganese Oxides

Oxalates ($Fe_{1-\alpha}Mn_\alpha C_2O_4$, $2H_2O$)	Oxides ($Fe_{3-x}Mn_xO_4$)[a]
$Fe_{0.93}Mn_{0.07}C_2O_4$, $2H_2O$	$Fe_{2.80}Mn_{0.20}O_4$
$Fe_{0.87}Mn_{0.13}C_2O_4$, $2H_2O$	$Fe_{2.60}Mn_{0.40}O_4$
$Fe_{0.73}Mn_{0.27}C_2O_4$, $2H_2O$	$Fe_{2.18}Mn_{0.82}O_4$
$Fe_{0.56}Mn_{0.44}C_2O_4$, $2H_2O$	$Fe_{1.67}Mn_{1.33}O_4$
$Fe_{0.44}Mn_{0.56}C_2O_4$, $2H_2O$	$Fe_{1.32}Mn_{1.68}O_4$
$Fe_{0.36}Mn_{0.64}C_2O_4$, $2H_2O$	$Fe_{1.08}Mn_{1.92}O_4$
$Fe_{0.22}Mn_{0.78}C_2O_4$, $2H_2O$	$Fe_{0.66}Mn_{2.34}O_4$

[a] $x = 3\alpha$.

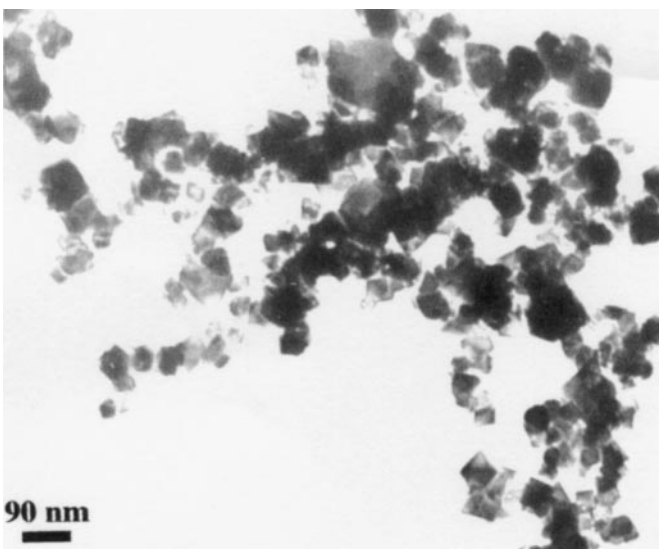

FIG. 2. TEM micrograph of an iron manganese oxide of composition $Fe_{2.18}Mn_{0.82}O_4$.

TABLE 2
Structure of Iron Manganites, $Fe_{3-x}Mn_xO_4$, Prepared at Different Temperatures

Temperature (°C)	Composition[a] (x)			
	1.33	1.68	1.92	2.34
410	C	C + T	T + C	T
430	C	C + T	T + C	T
450	C	C + T	T + C	T
470	C	C + T	T + C	T
500	C	C + T	T + C	T
530	C	C + T	T + C	T
1050	C	T	T + C	T

[a]C: cubic spinel. T: tetragonal spinel.

composition, the oxide has a cubic spinel structure (Fig. 3a), when it has been prepared undere precise conditions of temperature and of partial pressure of oxygen (the decomposition was done at 410°C under the mixture N_2/air, followed by annealing at 500°C under pure N_2). In contrast, the structure of the high-temperature phase (prepared in air at 1050°C and the reaction quenched) is tetragonal (Fig. 3b). Furthermore, the same manganite prepared respectively at 430 and 470°C is constituted of a mixture of cubic and tetragonal spinel phases. The relative intensity of the ratio of each phase changes with temperature. In fact, when the temperature was increased from 430 to 470°C, the ratio of the tetragonal phase increased (Fig. 3c and 3d).

Thermogravimetric analyses were performed (Fig. 4) to determine the oxygen content of the oxides. For different compositions and temperatures of thermal treatment, identical oxidation and reduction reactions are observed, but the mass change associated with the reaction varies. Four reactions are noticed during the heating ramp. The first pic appears at about 400°C, which is above the temperature of oxidation of Fe^{2+} in Fe^{3+} (200°C) (24), indicating that there is no Fe^{2+} cations in the structure. Since the oxides have been elaborated at a temperature equal or higher than 410°C in a mixture of N_2/air, it is not surprising that all the Fe cations are in the 3+ oxidation state. The gain of mass observed between 290 and approximately 425°C varies as a function of composition and calculation temperature. Earlier studies (24, 25) have shown that this reaction corresponds to the oxidation of the octahedral Mn^{3+} cations into Mn^{4+} cations. Gillot and Rousset (24) have pointed out, by studying the kinetics of the reaction, that the curve has a parabolic shape, i.e., that the structure did not transform. This oxidation leads to a nonstoichiometric spinel phase (with oxygen excess) $Fe_{3-x}Mn_xO_{4+\delta}$, δ being the nonstoichiometric coefficient. Above 425°C, the loss of mass observed is due to the reduction of the Mn^{4+} cations that were created at low temperature. The next reaction appears at 550°C and corresponds to the oxidation of the tetrahedral Mn^{2+} cations (26), and the spinel phase transforms into the cubic phase, α-$(Fe_yMn_{1-y})_2O_3$ (or into a mixture of α-Mn_2O_3 and α-Fe_2O_3 for iron-rich compounds). This observation is in agreement with the X-ray data, showing the appearance of the oxidized phase when the powders are obtained at a temperature higher than 560°C. In a few cases, a small drift of the TG signal is observed between 600 and 900°C. It probably corresponds to a shift of the baseline since no residual carbon or adsorbed water was detected by chromatography or by IR spectrometry (see the Experimental section). The last loss of mass noticed at high temperature (1000°C and above, as the iron content increases) is constant, approximately $3.1 \pm 0.2\%$, whatever the composition. The reaction is attributed to the reduction of the Mn^{3+} cations and leads to a phase transformation of $(Fe_yMn_{1-y})_2O_3$ into the stoichiometric spinel, as anticipated by the phase diagram, in agreement with Eq. [4]:

$$(Fe_yMn_{1-y})_2O_3 \rightarrow \tfrac{2}{3}\,Fe_{3-x}Mn_xO_4 + \tfrac{1}{6}\,O_2 \quad (\text{with } y = 2/3x). \qquad [4]$$

The theoretical mass loss associated with this reduction (3.3%) is close to the experimental one.

Finally, the difference of mass between the dwell at high temperature ($T \geq 1100$°C) corresponding to the stoichiometric phase and the dwell at low temperature ($T \approx 300$°C) corresponding to the initial defect spinel represents the oxygen excess and gives the coefficient of nonstoichiometry (δ) according to Eq. [5]:

$$Fe_{3-x}Mn_xO_{4+\delta} \rightarrow Fe_{3-x}Mn_xO_4 + \frac{\delta}{4}\,O_2. \qquad [5]$$

The value of δ and the temperature of stability of the stoichiometric spinel phase are reported in Table 3, as a function of iron content. The spinel phase is obtained at higher temperatures as the iron content increases, as predicted (4). The highest value of the nonstoichiometric coefficient δ, 0.4 per unit formula, was obtained for the oxides calcined at 410°C, and indicates a high ratio of cationic vacancies. The oxygen content is a little lower than the one corresponding to a defect spinel phase like γ-Mn_2O_3 or γ-Fe_2O_3 ($\delta = 0.5$). The manganese-rich compound $Fe_{0.66}Mn_{2.34}O_4$ is single phase (tetragonal spinel) at this temperature (410°C) and can be described as a solid solution between γ-Mn_2O_3 and γ-Fe_2O_3, of the chemical formula γ-$Fe_{0.44}Mn_{1.56}O_{2.93}$. A similar phase has been mentioned in the literature by Kolk *et al.* (27) and by Le Roux (28) in manganese ferrite prepared by continuous coprecipitation and calcined at temperatures below 600°C. The authors pointed out, in a powder of initial composition of

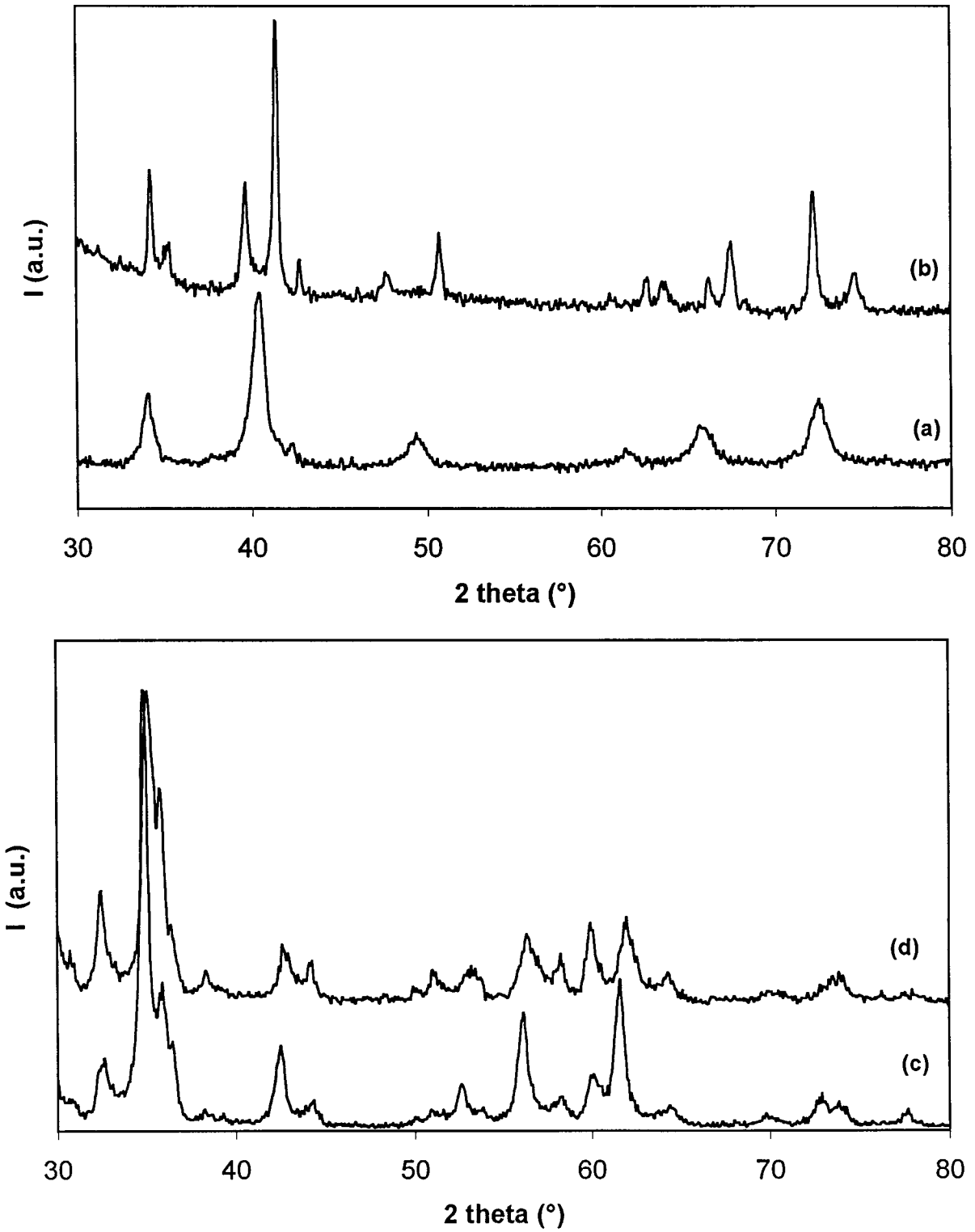

FIG. 3. X-ray diffraction pattern of an iron manganite of composition $Fe_{1.32}Mn_{1.68}O_4$ prepared at different temperatures: (a) 410°C (N_2/air) and annealed at 500°C (N_2); (b) 1050°C (air) and reaction quenched; (c) 430°C (N_2/air); (d) 470°C (N_2/air). **Note that* (*a*) *and* (*b*) *were obtained using CoKα wavelength while* (*c*) *and* (*d*) *were obtained using CuKα wavelength.*

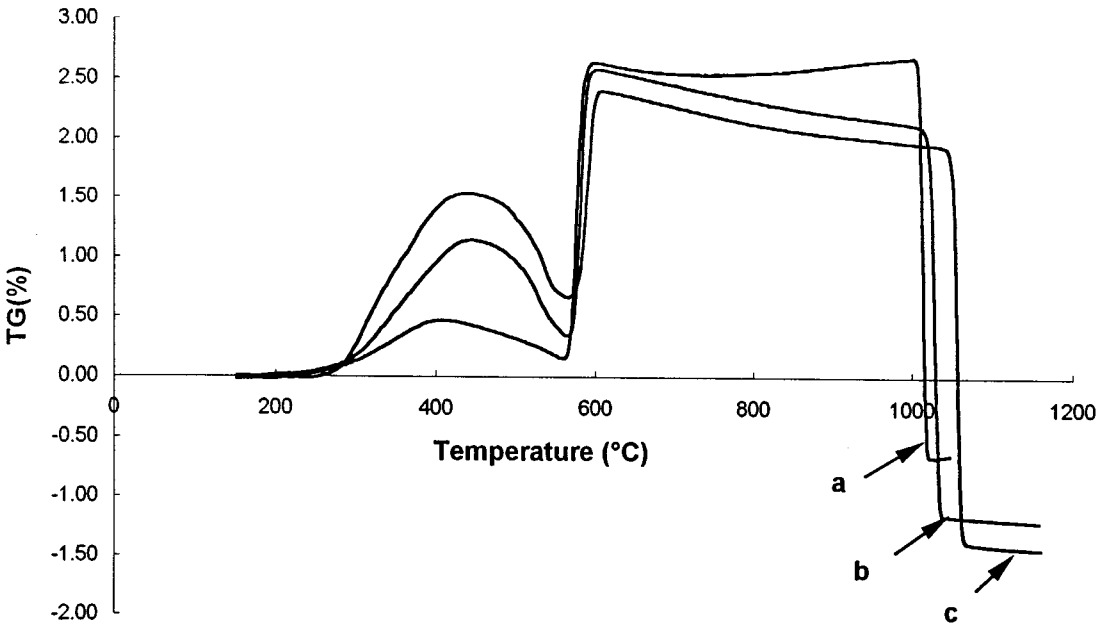

FIG. 4. Thermogravimetric analysis, under air flow, of iron manganites of composition: (a) $Fe_{0.66}Mn_{2.34}O_4$, (b) $Fe_{1.32}Mn_{1.68}O_4$, and (c) $Fe_{1.67}Mn_{1.33}O_4$ prepared at low temperature ($T = 410°C$).

$Fe_{1.9}Mn_{1.1}O_4$, the presence of two different magnetic phases. The paramagnetic component was described as a defect spinel phase of composition γ-$FeMnO_3$ while the magnetic phase is a Mn-substituted magnetite of composition $Mn_{0.6}Fe_{2.4}O_4$. Jimenez Mateos *et al.* (19) obtained a mixed iron manganese oxide with an oxygen-to-metal ratio ranging from 1.5 to 1.6. In this case, their samples would be more oxidized than γ-Fe_2O_3, which is arguable. We did not evidence, by X-ray diffraction analyses, a superstructure that could have been an indication of vacancies arrangements. However, the superstructure is generally only seen for iron-rich compounds of compositions ranging from Fe_3O_4 to $Fe_{2.36}Mn_{0.64}O_4$ (19).

TABLE 3
Temperature of Crystallization of the Stoichiometric Spinel Phase at High Temperature and Nonstoichiometric Coefficient δ, as a Function of the Composition and the Calcination Temperature, Determined by TGA

Composition	Calcination temperature (°C)	Temperature of crystallization of the stoichiometric spinel phase	Non-stoichiometry coefficient δ
$Fe_{1.67}Mn_{1.33}O_4$	410	1080	0.40
	410 + annealing (N_2) 500		0.20
	450		0.21
$Fe_{1.32}Mn_{1.68}O_4$	410	1060	0.43
	410 + annealing (N_2) 500		0.17
	420		0.21
	430		0.09
	1050		0.05
$Fe_{1.08}Mn_{1.92}O_4$	410	1050	0.30
	410 + annealing (N_2) 500		0.16
	470		0.01
$Fe_{0.66}Mn_{2.34}O_4$	410	1030	0.40
	410 + annealing (N_2) 500		0.17
	430		0.20
	450		0.10
	470		0.09

There is no regular evolution of the nonstoichiometric coefficient with iron content. However, δ strongly depends on the temperature of the thermal treatment. For example, the value of δ is divided by a factor of 2 when the temperature is increased 10°C only, for the composition $Fe_{1.32}Mn_{1.68}O_4$. In the same manner the oxide $Fe_{1.08}Mn_{1.92}O_4$ has an oxygen excess of 0.30 at 410°C while it is stoichiometric ($\delta = 0.01$) at 470°C. Whatever the composition, the maximum value of δ is obtained for a calcination temperature of 410°C. For lower temperatures, the crystallinity of the oxides is too poor for structural analysis, and no TG experiments were performed. The temperature of 410°C corresponds to the one of oxidation of Mn^{3+} cations into Mn^{4+} which leads to the formation of vacancies as described by

$$4Mn^{3+} \rightarrow 3Mn^{4+} + \square. \qquad [6]$$

Some powders, after being calcined at 410°C under a mixture of air/N_2, were annealed under pure nitrogen to increase the crystallinity of the oxide. The increase of the temperature, even realized under flowing neutral gas, causes

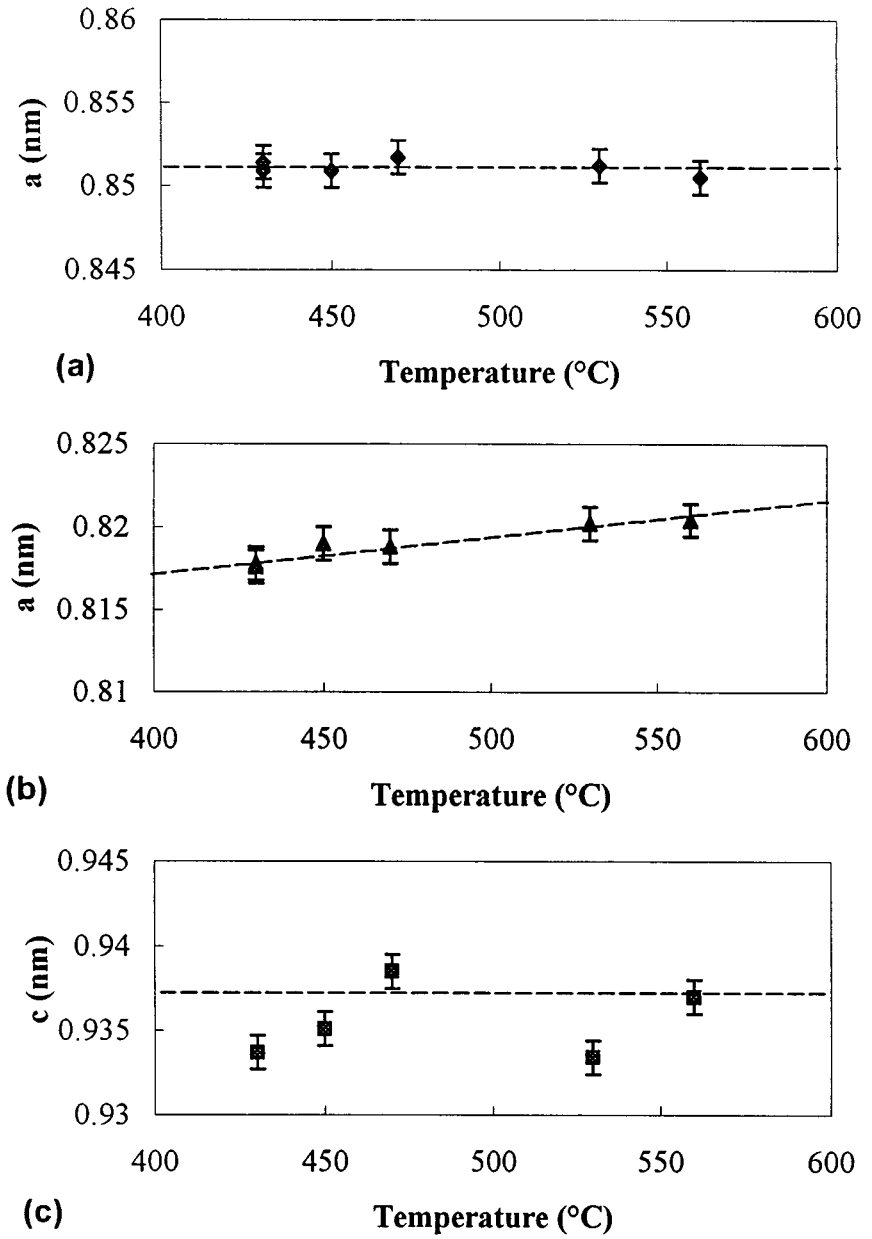

FIG. 5. Variation of the lattice parameters of the cubic phase (a) and of the tetragonal phase (b) and (c) as a function of temperature for the oxide of global composition, $Fe_{1.32}Mn_{1.68}O_4$.

a decrease of δ (Table 3). The modification of the oxygen content leads to a structural evolution, particularly the ratio of the cubic phase and the tetragonal phase. The oxides synthesized in this work contain no Fe^{2+}. So the change in oxygen content (without structural change) is related to the amount of Mn^{3+} that has been oxidized into Mn^{4+}, according to Eq. [6]. The X-ray data have shown that the amount of the tetragonal phase increases (Fig. 4) when the calcination is increased from 430 to 470°C, i.e., during the reduction of Mn^{4+} in Mn^{3+}. Thus, the amount of the tetragonal phase increases as the number of distorted Mn^{3+} increases, due to the Jahn–Teller effect. The oxide $Fe_{1.32}Mn_{1.67}O_4$ obtained at 410°C and annealed at 500°C under N_2 has an oxygen excess of 0.17 per unit formula. In this case the structure is cubic, which indicates that the number of Mn^{3+} is not high enough to cause the cooperative John–Teller effect.

The structure of the oxides synthesized in this work corresponds to the one of the mineral vredenburgite. The mineral is formed at high temperature and at high pressure

(1). We show here that the same structure can be elaborated at low temperature ($T < 500°C$) and at ambient pressure, by thermal decomposition of a mixed precursor. The mineral is a mixture of tetragonal and cubic phases and corresponds to an equilibrium state. So the composition of each phase is fixed, and a variation of the global composition should be balanced by the amount of those phases. It seemed difficult to determine directly the chemical composition of the cubic and tetragonal phases. Rather, we calculate the lattice parameter of the cubic and the tetragonal phases for different calcination temperatures. The variation of the lattice parameters for the oxide of global composition $Fe_{1.32}Mn_{1.68}O_4$ is shown in Fig. 5. The parameter (a) of the cubic phase (Fig. 5a) does not vary in the whole temperature range, i.e., the composition of the phase is constant. The average value of the lattice parameter, 0.851 nm, is similar to the one given by Mason (1) (0.850 nm). In this case, the limit composition of the cubic phase is very close to $Fe_{1.35}Mn_{1.65}O_4$, corresponding to the iron-rich side of the solubility limit of vredenburgite. For the tetragonal phase, the parameter (a) (Fig. 5b) increases slowly from 0.818 to 0.820 nm, that is, a little higher than the literature data, 0.817 nm (1). The higher value of (a) may indicate that the composition of the tetragonal phase is poorer in manganese than the one reported in (1). It means that the limit composition of the tetragonal phase determined in this work would be shifted toward FeO_4. The parameter (c) (Fig. 5c) shows a nonregular evolution, which is difficult to explain at this point. However, it oscillates around 0.935 nm (the same value as the one determined by Mason). According to these data, the limit composition of the tetragonal spinel phase is close to $Fe_{0.27}Mn_{2.73}O_4$, corresponding to the "right" side (Mn_3O_4) of the solubility limit. The evolution of the parameters probably has to do with the oxygen excess of the synthesized phases, contrary to the mineral, described as stoichiometric. Thus, the oxygen content of the oxides has to be considered as an additional parameter for the immiscibility gap, in the low-temperature range of the Mn_3O_4–Fe_3O_4 phase diagram.

CONCLUSION

Manganese iron oxides $Fe_{3-x}Mn_x\square_{3\delta/4}O_{4+\delta}$ were obtained at low temperature ($410 \leq T \leq 530°C$) by the decomposition of mixed oxalate precursors. The structure of the oxides depends on the iron content. On the manganese-rich side, for the compositions ranging from $Fe_{1.32}Mn_{1.68}O_4$ to $Fe_{1.08}Mn_{1.92}O_4$, the oxides are constituted of a mixture of cubic and tetragonal phases. The ratio of each phase depends on the temperature and on the oxygen partial pressure. The structure of these iron manganites prepared at low temperature is the same as the one of the mineral vredenburgite. The values of the lattice parameters of the cubic and tetragonal phases determined in this work confirm that the composition of each phase is fixed and corresponds to the solubility limits of the Fe_3O_4/Mn_3O_4 mixture. These low-temperature phases are defect spinel structure. The nonstoichiometry coefficient determined by TGA is approximately 0.4 per limit formula for the phases prepared at 410°C. Because of the small crystallite size, the oxidation of iron and manganese cations occurs at low temperature without structural changes and the nonstoichiometric coefficient is high.

ACKNOWLEDGMENTS

The authors thank L. Datas and J. J. Demai for the local analyses using the microprobe and C. Drouet for doing the chromatography and IR measurements.

REFERENCES

1. B. Mason, *Geol. Fören. Föreh. Stockholm Föerh* **65,** 97 (1943).
2. H. F. Mc Murdie, B. M. Sullivan, and F. A. Maur, *Natl. Bur. Standards J. Res.* **45,** 35 (1950).
3. H. J. Van Hook and M. L. Keith, *Am. Mineral.* **43,** 69 (1958).
4. A. Muan and S. Somiya, *Am. J. Sci.* **260,** 230 (1962).
5. D. G. Wickham, *J. Inorg. Nucl. Chem.* **31,** 313 (1969).
6. B. Von Punge-Witteler, *Z. Phys. Chem.* **143,** 239 (1984).
7. T. Tsuji, Y. Asakura, T. Yamashita, and K. Naito, *J. Solid State Chem.* **50,** 273 (1991).
8. M. O'Keefle, *J. Phys. Chem. Solids* **21,** 172 (1961).
9. G. C. Maiti, R. Malessa, and M. Baerns, *Appl. Catal.* **5,** 151 (1983).
10. G. C. Maiti, R. Malessa, U. Lochner, H. Papp, and M. Baerns, *Appl. Catal.* **16,** 215 (1985).
11. L. Cervinka, R. Hosemann, and W. Vogel, *Acta Crystallogr. A* **26,** 277 (1969).
12. P. Holba, M. A. Khilla, and S. Krupicka, *J. Phys. Chem. Solids* **34,** 387 (1973).
13. C. Vilette, Ph. Tailhades, and A. Rousset, *J. Solid. State Chem.* **117,** 64 (1995).
14. Ph. Tailhades, B. Gillot, and A. Rousset, *J. Phys. IV France* **7,** C1, 249 (1997).
15. L. Bouet, Ph. Tailhades, M. Durand, and A. Rousset, *J. Phys.* **7,** 523 (1997).
16. B. Gillot and M. El Guendouzi, *React. Solids* **1,** 139 (1986).
17. B. Gillot, M. El Guendouzi, and A. Rousset, *J. Solid State Chem.* **68,** 285 (1987).
18. B. Gillot, M. El Guendouzi, M. Laarg, Ph. Tailhades, and A. Rousset, *J. Mater. Sci.* **23,** 3342 (1988).
19. J. M. Jimenez Mateos, W. Jones, J. Morales, and J. L. Tirado, *J. Solid. State Chem.* **93,** 443 (1991).
20. M. A. Denecke, W. Gunsser, G. Buxhbaum, and P. Kuske, *Mater Res. Bull.* **27,** 507 (1992).
21. S. N. Dolia, A. Krishnamurthy, B. K. Srivastava, and V. Ghose, *J. Phys.* **38,** 2, 171 (1992).
22. J. P. Lagier, Ph.D. Thesis, Paris, 1970.
23. Ph. Tailhades, Ph.D. Thesis, Toulouse, 1988.
24. B. Gillot and A. Rousset, *HCR Compr. Rev.* **1,** 69 (1984).
25. S. Fritsch, Ph.D. Thesis, Toulouse, 1995.
26. B. Gillot, M. Laarj, S. Kacim, T. Battault, R. Legros, and A. Rousset, *Solid State Ionics* **83,** 215 (1996).
27. B. Kolk, A. Albers, G. R. Hearne, and H. Le Roux, *Hyperfine Interact.* **42,** 1051 (1988).
28. H. Le Roux, *J. Phys.: Condens. Matter* **2,** 3391 (1990).